Rangin, C., Silver, E., von Breymann, M. T., et al., 1990
Proceedings of the Ocean Drilling Program, Initial Reports, Vol. 124

8. GEOLOGICAL RESULTS OF A PRE-SITE SURVEY FOR ODP DRILL SITES IN THE SE SULU BASIN[1]

R. Vollbrecht[2,3] and H. R. Kudrass[2]

ABSTRACT

Five potential ODP drill sites in the SE Sulu Basin were surveyed for morphology, heat flow, hydrocarbon content of surface sediments, and sedimentology of late Pleistocene to Holocene sediments. Five piston cores were recovered from water depths between 3634 and 4600 m. The pelagic sediments consist of nannofossil-foraminifer marl and are interbedded with carbonate-poor and carbonate-rich turbidites. Turbiditic intercalations are abundant in the deeper parts of the basin (below 4000 m), whereas they are rare in marginal settings (Core KL 67—Site 769). Core KL 78 (near Site 768) records fewer turbidites and a composition change since isotopic stage 5c. Pelagic sedimentation rates typically range between 52 and 66 mm/k.y., with a carbonate input of 11–21 $g \cdot m^{-2} \cdot yr^{-1}$. Indications of major carbonate dissolution are absent even at 4600 m water depth. Near Site 769 (Core KL 67), gravity sliding and slumping may have removed several portions of the late Pleistocene sediments.

INTRODUCTION

In the course of a pre-site survey of ODP drill sites during cruise SO 58, five sites in the SE Sulu Basin (Fig. 1) were investigated with respect to morphology (Figs. 2 and 3), heat flow, surface sediments, and hydrocarbon gases. Five piston cores with a total length of ca. 67 m were recovered at five sites (Table 1). In addition, Core KL 96 from *Sonne* cruise SO 49 is considered for comparison.

HYDROGRAPHIC CHARACTERISTICS

The Sulu Sea is a marginal oceanic basin with a maximum depth of more than 4900 m, which is completely enclosed by shallow sills except for two deeper channels. Marginal depths are less than 200 m, whereas the channels—one off Panay, the other one between Negros and Mindanao—have maximum sill depths of 420 and 250 m, respectively. Situated in the tropical monsoon region of the Indonesian Archipelago, the surface circulation of the Sulu Sea is largely driven by the seasonally reversing winds (Wyrtki, 1961). Surface waters exchange readily with those of the surrounding Celebes and South China seas, but the renewal of deep and intermediate waters only takes place through the deepest, northern channel that connects the Sulu Sea to the South China Sea (Frische and Quadfasel, this volume). Therefore, the hydrographic conditions of the deeper Sulu Sea differ remarkably from those of the western Pacific Ocean.

Most prominent is absence of a typical decrease of temperature with increasing depth below the warm surface water; instead, the waters below 1000 m down to 4900 m uniformly show a temperature of about 10°C (Wyrtki, 1961; Frische and Quadfasel, this volume). Although the dissolved-oxygen content of the deep water below 2500 m is low (< 1.9–2.0 mL/L), oxygenated conditions are established in the whole basin. Salinity and SiO_2 content likewise exhibit little variation below 2500-m depth and are low compared to the western Pacific deep water.

MORPHOLOGY AND STRUCTURAL FRAME

NW–SE seismic sections of the SE Sulu Basin (Hinz et al., 1987; Rangin, 1989) reveal several major structural and morphological elements. To the northwest, the Cagayan Ridge bounds the basin against the shallower NW Sulu Basin. At about 2200 fathoms (ca. 4000 m) depth, the steep eastern flank of the Cagayan Ridge abuts sharply against the turbidite plain of the Sulu Trench. Farther to the southeast, the Sulu Trench is paralleled on its eastern side by (1) the accretionary wedge associated with the northeastward subduction of the SE Sulu Basin, (2) the Sulu fore-arc basin, and (3) the Sulu fore-arc ridge.

Core station KL 67 (Fig. 2) is situated between the Cagayan Ridge and Sulu Trench on a terrace high on the southeastern slope of a small, more or less isolated ridge. Station KL 69 lies on an even, gently eastward-sloping seafloor, much closer to the axis of the turbiditic Sulu Trench basin (Fig. 3). Cores KL 78 and KL 80 were taken on the basin plain further to the south. The latter two stations are separated by a shallow, east to west-trending sill. East of the Sulu Trench, core station KL 82 is located on the eastern flank of a NNE-trending ridge within the accretionary wedge which, as a whole, is forming a belt of roughly parallel, narrow basins and ridges.

About 150–200 km farther to the southwest (Fig. 1), core station KL 96 (SO 49) is situated at the transition from the southeast slope of Cagayan Ridge to a minor basin plain above the floor of the Sulu Trench proper.

HEAT FLOW

Heat-flow data from the seafloor clearly correlate with the overall structural pattern. They range from anomalously high (KL 69) to moderate (KL 80, KL 78) to low (KL 82, KL 67) values (Block and Steinmann, 1989; see Table 2).

On account of the very high heat flow at proposed site SS 1 (KL 69), this initially favored site was removed for safety reasons from the ODP schedule.

HYDROCARBON GASES

The results of *Sonne* cruise SO 49 pointed to a possibly high potential of hydrocarbon gases adsorbed in the surface sediments. Cruise SO 58 was expected to yield further information about the nature and origin of these gases. In the cores in question, however, gas concentrations (max. 33.7 ppb CH_4) do not exceed background (Berner et al., this volume).

---

[1] Rangin, C., Silver, E., von Breymann, M. T., et al., 1990. *Proc. ODP, Init. Repts.*, 124: College Station, TX (Ocean Drilling Program).

[2] Bundesanstalt für Geowissenschaften und Rohstoffe, Stilleweg 2, P.O. Box 510153, D-3000 Hannover 51, Federal Republic of Germany.

[3] Now at University of Göttingen, Department of Sedimentary Geology, Goldschmidtstr. 3, D-3400, Göttingen, Federal Republic of Germany.

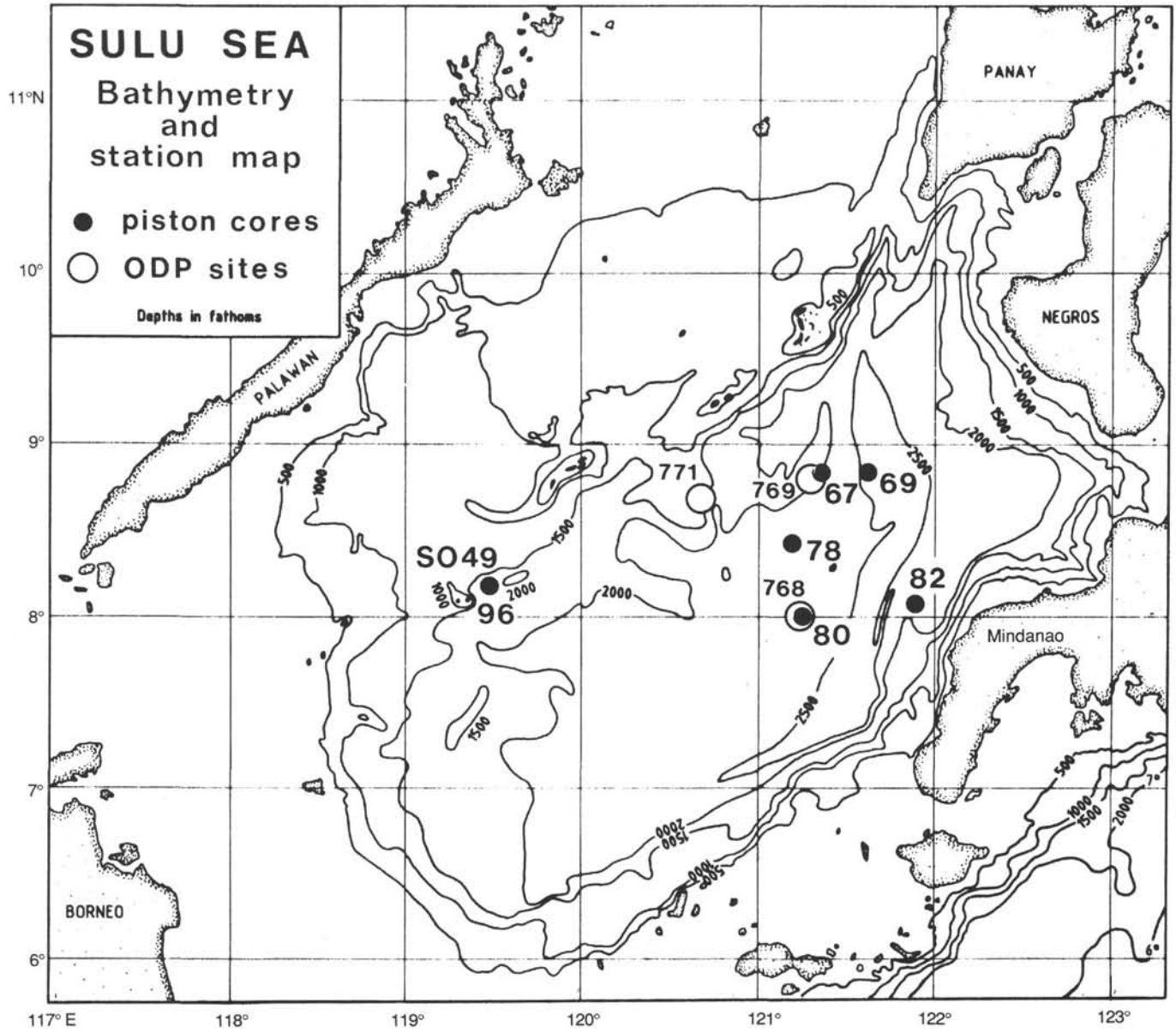

Figure 1. Map of the Sulu Sea region, showing locations of piston cores and ODP sites.

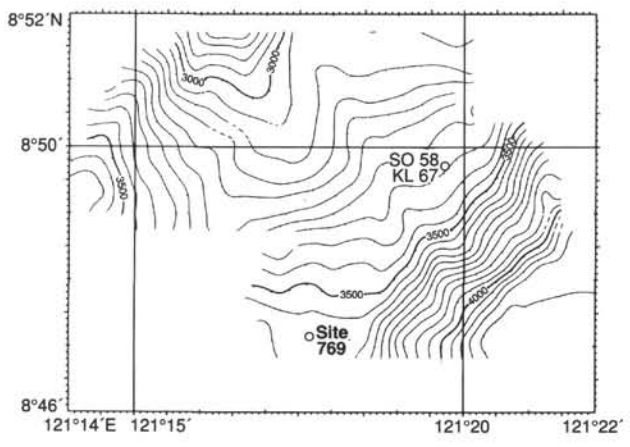

Figure 2. Bathymetry and station map (KL 67, Site 769). Contour interval is 50 m.

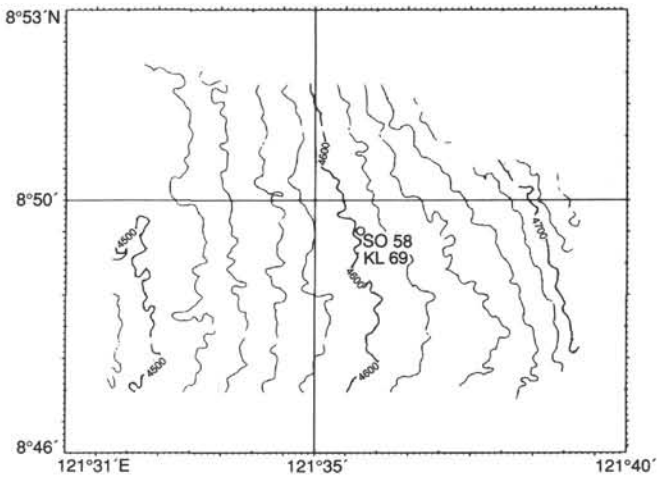

Figure 3. Bathymetry and station map (KL 69). Contour interval is 20 m.

Table 1. Core station locations.

Sonne cruise	Core	Position	Water depth (m)	Core recovery (cm)
SO 49	KL 96	E 119°28.0′ N 8°11.1′	3634	1313
SO 58	KL 67	E 121°19.7′ N 8°49.7′	3350	1257
	KL 69	E 121°35.7′ N 8°49.5′	4600	1372
	KL 78	E 121°10.7′ N 8°23.5′	4341	1436
	KL 80	E 121°14.4′ N 8° 0.2′	4313	1236
	KL 82	E 121°52.5′ N 8° 4.0′	3827	1370

Table 2. Heat flow data from the *Sonne* pre-site survey.

Core	Heat flow (mW/m^2)	
KL 69	154	
KL 80	108	Site 768
KL 78	94	
KL 82	54	
KL 67	32	Site 769

DOWNCORE RESULTS

Facies

The pelagic sediments consist of olive-gray (HUE 5Y 6/2) foraminifer-nannofossil marl and are intensely bioturbated. Brown colors (associated with oxygenated conditions) appear only in the uppermost 50–100 cm of each core. The average carbonate content is 35 wt.%, ranging from 25 wt.% (KL 82) to 40 wt.% (KL 67). There is no significant correlation between water depth and carbonate content in the studied cores; signs of strong dissolution are missing throughout. The sand fraction averages 14 wt.% of total sediment. Pelagic foraminifers and especially coccoliths are the most important calcareous components. Siliceous sponge needles and radiolarian tests usually occur only in minor amounts. Fecal pellets with an average diameter of about 75 μm are common.

Sediments of this pelagic foraminifer-nannofossil-facies comprise the whole of Core KL 67 (Fig . 4). Holocene (above ~ 1 m) and latest Pleistocene sediments in the uppermost portion of the core are separated by two discontinuities (185 and 310 cm, respectively) from underlying, slightly consolidated Pleistocene oozes of similar composition. These Pleistocene sediments bear *Globigerinoides ruber* pink (Fig. 5) and are thus older than about 120 ka, the subspecies' time of extinction in the Pacific (Thompson et al., 1979). Burrows filled with dark volcanoclastic material (glass, crystals) are common in the lower section of the core (below ~ 6 m), possibly indicating episodic winnowing of nearby volcanic outcrops. Radiolarian tests and siliceous sponge needles are remarkably abundant from 11.15 to 11.55 m core depth.

The pelagic portions of the cores from the Sulu Trench and the accretionary wedge closely resemble the sediments described above (Fig. 4). The average carbonate and sand contents, however, are usually some percent lower than in Core KL 67. Turbidite sequences, most of which are distal turbidites of different composition and thickness, intercalate with the pelagic material. Their carbonate and sand contents often greatly exceed those of the pelagic sediments. A typical turbidite comprises:

1. A basal sandy layer that is sometimes less than 1 mm thick (max 2.7 m) and composed of reworked planktonic foraminifers, volcanoclastic and/or siliciclastic material;
2. A medium layer of fine sand to silt with a distinct lamination that is visible only in radiographs; and
3. An upper layer of clay, usually free of sand and silt and colored darker than pelagic marls, in the uppermost parts commonly bioturbated from above (Wetzel, 1983). Carbonate content is often very low (Linsley et al., 1985).

Due to rapid burial, aragonitic remains (pteropod shells, ascidian spicules, otoliths) are preserved in turbidites well below the aragonite compensation depth (1400 m; Exon et al., 1981). Based on differences in coloration, two types may be distinguished:

1. White, light gray, or pale olive turbidites; and
2. Dark gray to dark olive turbidites.

Calcareous turbidites with a coarse fraction consisting mainly of foraminifers and detrital carbonate are often light-colored, whereas the others, with coarse fractions composed of volcanic glass and crystalline detritus, usually appear dark. Nevertheless, colorless volcanic glasses may well constitute the coarse fraction of light-colored turbidite layers.

Mud turbidites, which are commonly colored dark olive gray, are supposed to represent the most distal turbidite facies of one or both of the turbidite types described above.

Turbidites constitute a large portion of the sediment pile in all cores except for KL 67. Therefore, they contribute decisively to high sedimentation rates, e.g., as observed in Cores KL 80 and KL 82 (see below). Corrected for the turbidite influx, the calculated pelagic sedimentation rates are comparable throughout (Table 3).

The cores of the basin plain are distinguished quite clearly as to their pattern of turbidite abundance (Fig. 4). Core KL 78 starts with numerous, small turbidite layers 1–3 mm thick, that are replaced upward (above 10 m core depth) by frequent, thicker layers. Above 4 m core depth there is another increase in turbidite thickness also coupled with a decrease in turbidite frequency. Also, the abundance of carbonate-rich turbidites increases remarkably. There are 151 individual turbidite events recorded in Core KL 78. However, the actual number of events should be even higher, as the Holocene to latest Pleistocene sediments are missing due to trigger core failure. With respect to the frequency distribution of turbidite layers, Cores KL 78 and KL 69 are quite similar in appearance. Core KL 80, in contrast, shows less periodic and less abundant turbidite intercalations. Thicknesses of turbidites vary irregularly from a few millimeters to 2.6 m. Core KL 96 resembles Core KL 80 in turbidite abundance and appearance, although the maximum turbidite thickness is much lower in Core KL 96. Its lower section (below 860 cm) consists of a huge mass flow unit with an associated turbidite. Core KL 82 displays a rhythmic influx type with numerous, thin intercalations of mud turbidites. Based on the isotopic data (discussed later), there is a general tendency for turbidite events to concentrate around the transitional intervals between interglacial and glacial periods (see below) rather than on the more stable, interglacial or glacial periods themselves.

Stable Isotopes

Planktonic (*Globigerinoides ruber* white) $\delta^{18}O$ and $\delta^{13}C$ data were collected from pelagic units of all cores except KL 69. In parts, some of the cores (KL 78, KL 80) show considerable short-term isotopic variation. In addition to the isotopic analyses, we tried to confirm the position of the Pleistocene-Holocene transition by biostratigraphical means; i.e., by recognizing

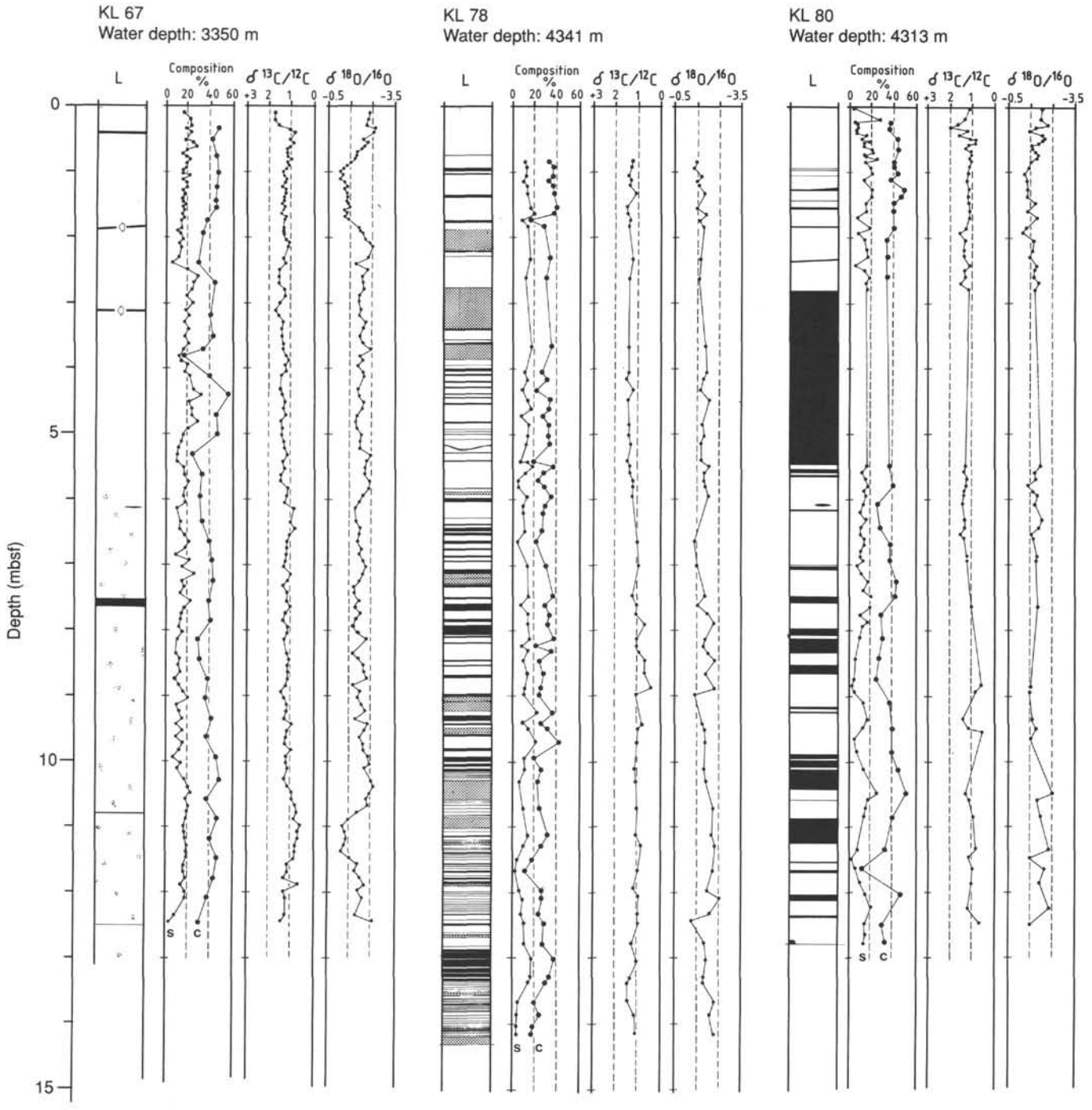

Figure 4. Sedimentary units and physical properties (pelagic portion) of Cores KL 67, KL 78, and KL 80. Lithology ("L"): White = pelagic sediment; black = carbonate-poor turbidite; stippled = carbonate-rich turbidite; hatched = disturbed by coring; arrow = discontinuity; point cluster (only KL 67) = ash-filled burrows. Composition: "c" = carbonate content (wt. %); "s" = sand content (wt. %). $\delta^{13}C/^{12}C$ and $\delta^{18}O/^{16}O$ also shown.

the last appearance of *Globoquadrina crassaformis*. This species disappeared in the Sulu Sea at or around the time of the last glacial maximum (18 ka; Linsley et al., 1985), an assumption that is supported by the findings in those of our cores with more clearly defined isotopic trends (KL 67, KL 82, KL 96).

The range of $\delta^{18}O$ values is comparable throughout, with about $-1.2‰$ for the last glacial maximum and $-2.7‰$ for interglacial conditions. If we assume that the 18-ka datum is characterized by a coincidence of the most positive $\delta^{18}0$ values with the extinction of *G. crassaformis*, sedimentation rates for this time interval may be calculated (Table 3). Cores KL 67 and KL 96 are almost purely pelagic in the section in question and yield sedimentation rates of 55 and 53 mm/k.y., respectively. The somewhat higher total sedimentation rates of Cores KL 80 and KL 82 are caused by minor contributions of turbidites. In comparison, the turbiditic input into the central Sulu Trench is

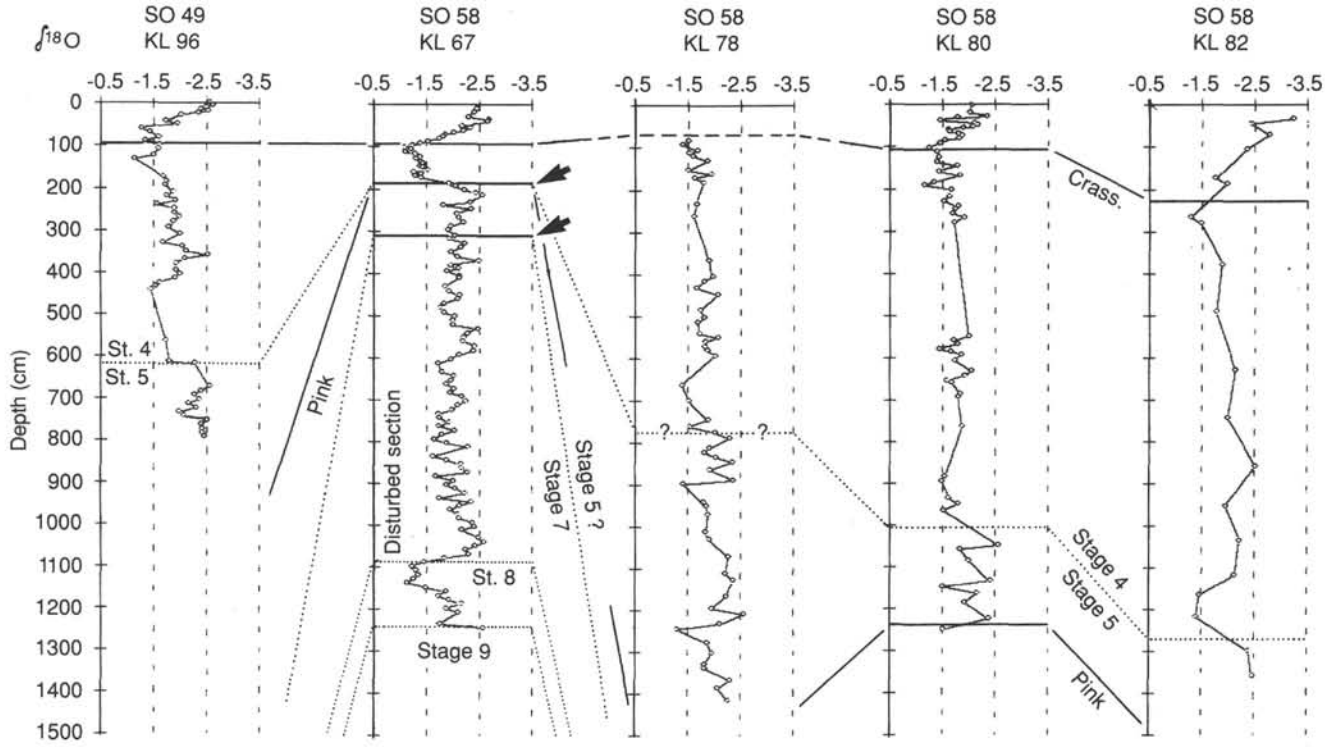

Figure 5. Interpretation of biostratigraphic and $\delta^{18}O$ isotopic data. Arrow = discontinuity; "pink." = disappearance of *Globigerinoides ruber* pink; "crass." = disappearance of *Globorotalia crassaformis*.

Table 3. Calculated total and pelagic sedimentation rates.

Core	Section (cm)	Total rate (mm/k.y.)	Pelagic rate (mm/k.y.)	Pelagic accumulation rate bulk ($g \cdot m^{-2} \cdot yr^{-1}$)	Pelagic accumulation rate carbonate ($g \cdot m^{-2} \cdot yr^{-1}$)
KL 96	0–95[1]	53	53	≥ 28	
	95–674	95	54	≥ 29	
KL 67	0–99.5[1]	55	55	25	21
	310–1080[2]	154	151	85	33
	1080–1241[3]	28	28	16	7
KL 78	750–1436	≃ 124	≃ 87	≃ 46	≃ 13
KL 80	0–108[1]	60	52	27	11
	108–1238	111	66	35	13
KL 82	0–228[1]	125	114	≥ 59	≥ 14
	228–1218.5	210	174	≥ 92	≥ 23

[1] Core section younger than 18 k.a.
[2] Presumably isotopic stage 7 } sedimentation rates
[3] Presumably isotopic stage 8 } not reliable

about 10–20 times higher (Exon et al., 1981). Corrected for the turbiditic influence, however, the (pelagic) sedimentation rate calculated for Core KL 80 is 52 mm/k.y. As a whole, these results suggest a pelagic sedimentation rate in the range of 52–55 mm/k.y. Based on the average dry-bulk density of latest Pleistocene to Holocene sediments (0.46–0.52 g/cm^3, Tables 4 and 5), this may be expressed as a rate of 24–29 g sediment/m^2/year. Nevertheless, Core KL 82 is an obvious exception with a calculated pelagic sedimentation rate of 114 mm/k.y.

Sedimentation rates may be calculated also for the Pleistocene section older than 18 ka of Core KL 80 by using the last appearance of *G. ruber* pink. In this core, *G. ruber* pink is present only in the two lowermost samples. Therefore, a total sedimentation rate of 111 mm/k.y. and a pelagic sedimentation rate of 66 mm/k.y. is calculated for the period between 18 and 120 ka. Unfortunately, adequate lower time marks are missing in the Pleistocene portion of the other cores, so that an evaluation of sedimentation rates is possible only by comparing the oxygen isotopic record to published curves from other areas (Shackleton and Opdyke, 1973; Sarntheim et al., 1984; Martinson et al., 1987). The oxygen isotope curve of Core KL 96 (Fig. 5) exhibits a negative peak between 600 and 750 cm, which is thought to represent isotopic stage 5a (maximum ^{18}O-depletion at 79 ka; Martinson et al., 1987). Correspondingly, the total pelagic sedimentation rates for the time span from 18 to 79 ka would be 95 and 54 mm/k.y., respectively. Thus, Cores KL 80 and KL 96 yield pelagic sedimentation rates for the late Pleistocene that agree well with the ones calculated for the time since the last glacial maximum.

Core KL 82 is characterized by a $\delta^{18}O$ shift toward more positive values, presumably corresponding to isotopic stage 4 (maximum at about 65 ka), around 1200 cm core depth. In this case, the calculated pelagic sedimentation rate of 174 mm/k.y. for the Pleistocene portion older than 18 k.y. is even higher than the estimation of 114 mm/k.y. calculated for the subsequent period (Table 3).

For Core KL 67, oxygen and carbon isotopic and foraminifer data (*G. ruber* pink present) indicate that the section below 310 cm comprises isotopic stage 8 and the lower part of isotopic stage 7. If this is so, then the pelagic sedimentation rate for the isotopic stage 8 would be ~ 28 mm/k.y., in contrast to an estimated minimum rate of more than 150 mm/k.y. for the recorded part of isotopic stage 7. The great divergence of sedimentation rates indicates the problematic nature of this stratigraphic classification. The interpretation of the oxygen isotopic signal of Core KL 78 is even less straightforward (see above). Nevertheless, the recovered sediments seem to represent the time span from the end of isotopic stage 5e to an early phase of the last glacial maximum. This would indicate, in rough approximation, a pelagic sedimentation rate somewhat increased above the average level of 52–66 mm/k.y.

Table 4. Porosity, bulk density, and water content of pelagic sediments in Core KL 67.

Depth in core (cm)	Porosity (%)	Dry-bulk density (g/cm^3)	Wet-bulk density (g/cm^3)	Water content (%)	Carbonate content (%)
35	79.8	0.44	1.26	172.2	47.2
52	79.8	0.45	1.27	169.9	41.6
77	78.4	0.50	1.30	150.8	45.6
102	82.4	0.50	1.34	157.9	47.4
146	83.5	0.51	1.36	158.0	45.3
156	81.1	0.50	1.33	156.3	45.6
174	81.8	0.48	1.32	163.7	37.3
195	82.9	0.45	1.30	176.5	33.1
240	82.5	0.46	1.30	171.4	29.2
270	78.5	0.52	1.32	145.6	44.5
320	78.8	0.48	1.29	158.2	40.4
352	77.3	0.53	1.32	139.9	43.5
362	78.4	0.51	1.31	132.4	
372	78.4	0.51	1.31	148.4	33.5
382	68.4	0.75	1.45	89.0	16.1
390	77.7	0.52	1.32	143.6	
413	73.7	0.63	1.39	113.5	39.3
443	76.0	0.54	1.32	134.6	56.9
473	74.9	0.55	1.32	130.5	45.6
503	77.8	0.58	1.38	129.0	47.2
533	72.3	0.66	1.40	106.7	24.8
563	73.2	0.60	1.36	117.2	33.5
595	75.7	0.62	1.40	117.2	31.4
635	81.1	0.48	1.31	162.6	33.3
665	77.2	0.51	1.30	144.8	39.9
695	83.5	0.51	1.36	155.6	42.2
726	79.0	0.52	1.33	147.0	43.1
756	73.9	0.62	1.38	115.8	39.1
785	78.5	0.51	1.31	148.2	41.4
815	80.7	0.53	1.36	146.3	29.1
845	77.1	0.52	1.31	142.4	31.0
875	80.6	0.48	1.31	159.5	38.5
905	79.0	0.56	1.37	136.8	36.4
937	79.2	0.55	1.36	139.1	42.0
965	74.6	0.60	1.36	120.6	37.0
995	77.4	0.55	1.34	135.6	45.8
1030	78.2	0.56	1.36	135.4	49.2
1060	76.5	0.59	1.37	125.2	37.4
1090	75.1	0.56	1.33	129.9	47.5
1120	73.6	0.69	1.45	103.3	40.6
1150	76.8	0.59	1.38	125.5	46.8
1180	78.4	0.51	1.31	147.9	43.7
1210	75.6	0.54	1.31	135.0	37.6
1246	78.0	0.47	1.27	157.3	30.5

The last post-glacial carbon isotopic record shows a similar pattern throughout. There is a shift from glacial (isotopic stage 2) values around 1.25% toward more negative values (~ 0.8%) in the early Holocene, followed by a trend to more positive values (ca. 1.6–2.0%). A renewed shift toward more negative values is recorded in the uppermost Holocene sediments of two cores (KL 80, KL 82), but in neither case are the corresponding samples unequivocally free of reworked material.

For the Pleistocene, enrichment in lighter carbon often coincides with colder periods, but the most prominent peaks usually correlate with the transitional phases from glacial to interglacial conditions (e.g., Core KL 67). Otherwise, two cores have recorded ^{13}C-depleted peaks for the periods interpreted as isotopic stage 5a (Core KL 78) and its transition to stage 4 (Core KL 80), respectively.

DISCUSSION

The range of calculated sedimentation rates corrected for turbiditic influx (52–66 mm/k.y.) is in accord with the values that may be evaluated from the data of Linsley et al. (1985). Their two cores from the SE Sulu Basin show sedimentation rates of about 55 and 65 mm/k.y. for the period since the last glacial maximum (Linsley et al., 1985; Figs. 10 and 11). Based

Table 5. Porosity, bulk density, and water content of pelagic sediments in Core KL 80.

Depth in core (cm)	Porosity (%)	Dry-bulk density (g/cm^3)	Wet-bulk density (g/cm^3)	Water content (%)	Carbonate content (%)
25	81.5	0.47	1.31	164.9	36.4
35	79.7	0.48	1.30	158.1	35.0
50	81.1	0.49	1.32	159.4	42.7
65	78.8	0.55	1.36	137.9	43.7
85	75.5	0.58	1.36	124.7	39.8
93	72.8	0.58	1.32	121.6	39.8
103	80.2	0.49	1.32	155.5	43.3
113	81.3	0.54	1.37	145.7	36.6
127	86.2	0.48	1.36	171.0	49.7
138	77.0	0.54	1.33	136.2	46.0
148	80.8	0.50	1.33	155.4	39.3
160	80.4	0.51	1.33	151.9	40.0
170	82.0	0.46	1.30	171.4	
186	80.5	0.50	1.32	154.8	40.0
193	81.9	0.47	1.32	164.7	
204	79.2	0.46	1.27	165.5	33.5
220	82.5	0.43	1.28	181.3	
230	80.5	0.50	1.32	154.5	34.3
243	74.5	0.59	1.35	122.9	
250	80.5	0.50	1.33	153.4	
261	78.2	0.46	1.27	161.2	34.3
270	79.8	0.54	1.36	142.5	
280	81.7	0.46	1.30	169.0	
550	82.5	0.54	1.38	147.5	36.8
560	69.7	0.49	1.20	137.6	
570	76.2	0.62	1.41	118.3	
580	75.1	0.56	1.33	130.1	40.4
588	75.6	0.60	1.38	120.8	
595	77.4	0.63	1.42	119.0	
608	69.4	0.77	1.48	88.4	25.3
620	77.4	0.51	1.30	146.1	
632	76.7	0.57	1.35	130.6	
644	77.9	0.56	1.35	134.9	27.8
655	77.3	0.67	1.46	112.1	
661	77.5	0.54	1.34	136.8	
670	80.1	0.57	1.40	134.4	37.7
680	77.0	0.53	1.32	139.6	
688	80.1	0.47	1.29	162.6	
695	77.9	0.58	1.38	129.4	37.5
715	81.4	0.61	1.44	128.8	
727	81.4	0.49	1.32	159.2	43.8
740	68.8	0.73	1.43	91.9	
749	80.1	0.47	1.29	162.4	42.3
765	82.1	0.49	1.33	160.6	
777	81.0	0.55	1.38	142.5	28.8
787	80.3	0.51	1.34	149.7	
795	77.6	0.49	1.29	151.4	
812	83.2	0.42	1.28	186.2	31.0
844	78.8	0.54	1.35	139.9	27.0
875	80.4	0.50	1.32	155.2	24.6
885	79.2	0.42	1.23	180.6	
895	80.8	0.49	1.32	157.3	
911	79.1	0.53	1.34	144.0	37.7
936	77.7	0.56	1.35	134.8	
950	78.9	0.52	1.33	146.4	39.8
966	78.9	0.47	1.28	160.1	
986	84.2	0.49	1.36	163.3	39.0
1013	81.9	0.46	1.30	170.2	44.8
1050	78.5	0.56	1.37	134.8	52.4
1060	73.9	0.69	1.45	103.3	
1072	76.5	0.60	1.39	122.2	
1086	77.1	0.52	1.32	141.4	40.0
1135	81.5	0.50	1.33	157.3	33.1
1149	80.7	0.41	1.24	187.5	
1165	74.5	0.67	1.43	108.4	12.0
1187	80.5	0.48	1.30	161.3	
1204	83.4	0.47	1.32	170.1	47.4
1225	81.8	0.44	1.28	177.8	
1250	77.4	0.64	1.43	117.0	30.3
1265	82.2	0.50	1.35	156.4	
1278	80.0	0.48	1.30	159.9	33.3

on an average total sedimentation rate of ca. 110 mm/k.y. for the Pleistocene portion of our cores (Table 3), and using the corresponding mean dry-bulk density of 0.5 g/cm^3, a comparable sediment accumulation rate of ca. 55 g · m^{-2} · yr^{-1} is indicated. This, however, does not apply to Core KL 82, whose total and pelagic sedimentation rates exceed those of the other cores by a factor >2 due to a higher input from nearby terrestrial source areas.

The sedimentation rates calculated for the Pleistocene section of Core KL 67 below 185 cm are not reliable (Table 3). A considerable portion of the late Pleistocene sediments (isotopic stages 3, 4 and 6; parts of isotopic stages 2 and 5) may have been removed by gravity sliding. Two of these discontinuities are visible within the core, others might not be. This may be an explanation for the seemingly low sedimentation rates within the stage 8 interval. Elsewhere (stage 7 interval), slumping within the homogeneous sediments may have increased the unit's thickness, resulting in an extraordinarily high value for the sedimentation rate. Therefore, we interpret the recovered Pleistocene section below 185 cm core depth as a disturbed deposit.

$\delta^{13}C$ analyses of planktonic foraminifers reveal the same trends for the latest Pleistocene as those from the cores presented by Linsley et. al. (1985). According to their interpretation, which is supported by biostratigraphical results and paleoecological considerations, the transition to interglacial conditions at the end of the Wisconsin glaciation was characterized by low-salinity Sulu Sea surface water enriched in isotopically light carbon. Also, for most of the Pleistocene sediments cored by us, peaks of ^{12}C-enriched carbon either coincide with, or closely follow, peaks of ^{18}O-depleted oxygen; i.e., glacial phases. Following the model of Berger and Vincent (1986), the shift to ^{12}C-enriched values might be explained by a weaker biocarbon pumping, that is, a decreased surface production. Apparently, the processes relevant to the fractionation of carbon isotopes happened during the Pleistocene to Holocene transition as well as during Pleistocene glacial to interglacial transitions.

The slightly increased abundance of turbiditic layers in transitional intervals between the main isotopic stages possibly points to a climatic control similar to the one proposed by Weaver et al. (1983) for the Madeira Abyssal Plain. They presumed that turbidity currents were preferrentially released during the re-arrangement of shorelines and deltas in the course of great regressions and transgressions. In the case of the SE Sulu Sea Basin, however, this was certainly not the main controlling factor. Core KL 78, for example, reflects a change in depositional environment; i.e., from highly frequent, distal, carbonate-poor to proximal, carbonate-rich turbidites. Furthermore, turbidites are strikingly rare in the core sections younger than 18 k.y., just when they should be most common if climate were the main controlling influence (Table 3). Changes in the internal water-mass structure, fluctuations of sea level and of the rate of deep-water renewal via the South China Sea are possible mechanisms controlling the generation and intensity of turbidity currents. Thus, it seems that turbidite deposition in the SE Sulu Sea basin was a process restrained by local as well as global, climate-controlled parameters.

ACKNOWLEDGMENTS

The Bundesministerium für Forschung und Technologie (German Federal Ministry of Research and Technology) financed both *Sonne* cruises. We acknowledge the contribution of Dr. H. Erlenkeuser, Institut für Reine und Angewandte Kernphysik, Universität Kiel, who supplied isotopic analyses on planktonic foraminifers.

REFERENCES

Berger, W. H., and Vincent, E., 1986. Deep-sea carbonates: reading the carbon isotope signal. *Geol. Rundsch.*, 75:249–269.

Block, M., and Steinmann, D., 1988. Geothermal studies. *In* Kudrass, H.-R., et al. (Eds.), *Geological, Geochemical and Geothermal Investigations in the Sulu Sea/Philippines* (SO 58). BGR Rep. 104774, Pt. 2 (Hannover, F.R. Germany).

Exon, N. F., Haake, F.-W., Hartmann, M., Kögler, F.-C., Müller, P. J., and Whiticar, M. J., 1981. Morphology, water characteristics, and sedimentation in the silled Sulu Sea, Southeast Asia. *Mar. Geol.*, 39: 165–195.

Hinz, K., Fritsch, J., Kewitsch, P., Popovici, A., Roeser, H., and Wissmann, G., 1988. *In* Kudrass, H.-R., et al. (Eds.), *Geological, Geochemical and Geophysical Investigations in the Sulu Sea/Philippines* (SO 49). BGR Rep. 102042, Pt. 3 (Hannover, F. R. Germany).

Linsley, B. K., Thunell, R. C., Morgan, C., and Williams, D. F., 1985. Oxygen minimum expansion in the Sulu Sea, western equatorial Pacific, during the last glacial low stand of sea level. *Mar. Micropaleontol.*, 9:396–418.

Martinson, D. G., Pisias, N. G., Hays, J. D., Imbrie, J., Moore, T. C., Jr., and Shackleton, N. J., 1987. Age dating and the orbital theory of the ice ages: development of a high-resolution 0 to 300,000-year chronostratigraphy. *Quat. Res.*, 27:1–29.

Rangin, C., 1989. The Sulu Sea, a back-arc basin setting within a Neogene collision zone. *Tectonophysics*, 161:119–141.

Sarnthein, M., Erlenkeuser, H., von Grafenstein, R. and Schröder, C., 1984. Stable-isotope stratigraphy for the last 750,000 years: "Meteor" core 13519 from the eastern equatorial Atlantic. *"Meteor" Forschungsergeb., Reihe C*, 38:9–24.

Shackleton, N. J., and Opdyke, M. D., 1973. Oxygen isotope and palaeomagnetic stratigraphy of equatorial Pacific core V28-238: oxygen isotope temperatures and ice volumes on a 10^5 year to 10^6 year scale. *Quat. Res.*, 3:39–55.

Thompson, P. R., Bé, A.W.H., Duplessy, J. C., and Shackleton, N. J., 1979. Disappearance of pink-pigmented *Globigerinoides ruber* at 120,000 yr BP in the Indian and Pacific Oceans. *Nature*, 280:554–558.

Weaver, P.P.E., and Kuijpers, A., 1983. Climatic control of turbidite deposition on the Madeira Abyssal Plain. *Nature*, 306:360–363.

Wetzel, A., 1983. Biogenic structures in modern slope to deep-sea sediments in the Sulu Sea Basin (Philippines). *Palaeogeogr., Palaeoclimatol., Palaeoecol.*, 42:285–304.

Wyrtki, K., 1961. Scientific results of marine investigations of the South China Sea and the Gulf of Thailand 1959-1961. *NAGA Rep.*, 2.

Ms 124A-108